Nuclear Physics **A528** (1991) 203-214
North-Holland

THE BETA DECAY OF ^{48}Mn

Improved data on Gamow-Teller quenching

J. SZERYPO[1*], D. BAZIN[2], B.A. BROWN[3], D. GUILLEMAUD-MUELLER[4], H. KELLER[1], R. KIRCHNER[1], O. KLEPPER[1], D. MORRISSEY[1**], E. ROECKL[1], D. SCHARDT[1] and B. SHERRILL[3]

[1] *GSI Darmstadt, Postfach 110552, D-6100 Darmstadt 11, Germany*
[2] *CEN Bordeaux, Le Haut Vigneau, F-33170 Gradignan, France*
[3] *Michigan State University, Department of Physics and Astronomy, East Lansing, MI 48824, USA*
[4] *Institut de Physique Nucléaire, F-91406 Orsay Cedex, France*

Received 14 November 1990

Abstract: The very proton-rich nuclide ^{48}Mn, produced in ^{12}C(^{40}Ca, p3n) reactions, was investigated using on-line mass separation combined with singles and coincidence spectroscopy of β-delayed γ-rays and protons. Compared to the previous ^{48}Mn decay work, a more accurate value of 158.1 (22) ms was obtained for the half-life, γ singles, $\gamma\gamma$-coincidence and proton singles data were improved, and proton-γ coincidences were measured for the first time. A revised ^{48}Cr level scheme is proposed. The experimentally deduced Gamow-Teller strength distribution is compared with predictions from shell-model calculations.

E

RADIOACTIVITY ^{48}Mn [from ^{12}C(^{40}Ca, 3np)]; measured $T_{1/2}$, β-delayed, E_γ, I_γ, β-delayed, E_p, I_p, $\sigma\gamma$, pγ-coin; deduced log *ft*. ^{48}Cr deduced levels, Fermi and Gamow-Teller transition strength. Shell-model calculations. Ge, surface-barrier Si detectors. On-line mass separation.

1. Introduction

Beta-decay studies of very proton-rich nuclides have found renewed interest recently, since they allow, as a competing tool to charge-exchange reactions, to investigate the phenomenon of quenching of Gamow-Teller (GT) transitions. The quenching factor, defined as the ratio between measured and calculated GT transition strength, is used for a renormalization of the weak axial-vector coupling constant or of the calculated GT matrix elements; it therefore covers effects such as second-order configuration mixing, meson exchange, and isobar excitations, which are usually not taken into account in the underlying shell-model calculations.

Relevant to this question is, e.g., the first measurement [1]) of the beta decay of the very proton-rich 1p0f shell nuclide ^{48}Mn, which yielded an average GT quenching factor of 0.53 (17) for a 0-5.8 MeV interval of excitation energies in the daughter

* On leave of absence 1987-1989 from Warsaw University, Institute of Experimental Physics, PL-00681 Warsaw, Poland.

** On leave of absence 1987-1988 from Michigan State University, Department of Chemistry, East Lansing, MI 48824, USA.

nuclide ^{48}Cr. This value, which is based on shell-model calculations including 1p1h excitations, appears to be in good agreement with the global quenching factor of 0.58 (5) for the middle of the 1s0d shell [2]), and with the average quenching factor of 0.560 (54) for the 1p0f shell [3]). However, deviations from such a regular behaviour have been observed for neutron-deficient argon isotopes at the end of the 1s0d shell [4]), and for some of the ground-to-ground mirror transitions in the 1p0f shell [3,5,6]).

In order to improve the understanding of GT quenching, it seems thus appropriate to reduce the experimental uncertainties of GT strength values in general and, for cases such as ^{48}Mn, to increase the covered range of excitation energies in the daughter nuclide. In this paper, we describe a corresponding reinvestigation of the ^{48}Mn decay. We start out with a presentation of the experimental techniques (sect. 2). The results of the measurements are discussed, in comparison to shell-model calculations, in sect. 3.

2. Experimental techniques

The measurements were carried out at the GSI on-line mass separator, the techniques of production through $^{12}C(^{40}Ca, p3n)$ reactions, of reionization and of mass separation being similar to those used for the previous investigation [1]). For UNILAC beam currents of 120 particle nA, the intensity of the mass-separated ^{48}Mn beam was in the range between 200 and 600 atoms/s. This improvement in ^{48}Mn source strength was reached by applying the FEBIAD-B2-A ion source [7]). In order to suppress ^{48}Cr as a contaminant of mass-48 beams, the ion source was operated with a cold pocket during the initial part of the measurements. Since this operation mode also led to a decrease of the ^{48}Mn yield, an ion source without cold pocket was used later on.

The ^{48}Mn decay spectroscopy was performed simultaneously in two beam lines of the mass separator: One of them was equipped with a proton-$\gamma\gamma$ detector array, while the other one was devoted to half-life determination. At the end of both lines, tape collectors were mounted with the detectors viewing the position where the ^{48}Mn beam was implanted. Subsequent to a 1.70 s collection period for the proton-$\gamma\gamma$ measurements, the mass-48 beam was switched, by means of a horizontal electrostatic deflector in front of the separator magnet, for 0.40 s to the other beam line for the half-life measurement. The tape collectors moved the activity out of the detector position after fifty 2.10 s cycles in the former and after each 1.54 s counting period in the latter case.

The proton-$\gamma\gamma$ detector set-up consisted of two surface-barrier detector telescopes and two hyperpure germanium detectors. The telescopes (15.6 μm, 150 mm^2; 531 μm, 450 mm^2 and 17.3 μm, 150 mm^2; 541 μm, 450 mm^2) were mounted above and below the tape, leaving an opening for the passage of the ^{48}Mn beam. The detection efficiency of each of the telescopes was estimated from the geometry to be

(4.0 ± 0.4)%, and the energy resolution for low-energy protons was approximately 50 keV. Due to gain-shift problems, only one telescope was used to obtain a proton-energy spectrum from ΔE-E coincidence data, whereas both telescopes were applied for measuring proton-γ coincidences. The germanium detectors were positioned at 90° with respect to each other, and had absolute photopeak efficiencies with respect to the collection spot of 4.6% and 3.1%, respectively, for 1.3 MeV γ-rays. Using the GSI data acquisition system, GOOSY and VAX 8600 computers, coincidence data were recorded event by event, and single spectra were accumulated in multispectrum mode. From the multispectrum data, γ-rays were assigned to the ^{48}Mn decay due to their grow-in/decay characteristic, which was observed for the strongest lines; the main basis for this assignment, however, were the $\gamma\gamma$-coincidenes from this work combined with earlier results [1]).

For the accurate determination of the ^{48}Mn half-life, a hyperpure germanium detector was used for performing a multispectrum analysis with 64 subgroups of 1024 channels each and with counting-intervals of 24 ms per subgroup. An γ-energy range from 0 to 1.3 MeV was chosen in order to enable setting of photopeak and background windows in the off-line analysis of the 752 keV γ-ray which represents the strongest transition in the ^{48}Mn decay.

3. Results and discussion

Using a total counting time of approximately 50 h at the proton-$\gamma\gamma$ detector array, the statistics of the γ singles and coincidence data were improved roughly by 60% compared to the previous experiment [1]). The γ-spectra measured at mass-48 were again somewhat obscured by ^{48}Cr, ^{48}V, ^{48}Sc and ^{21}F contaminants, the latter one being due to the formation of $^{27}Al^{21}F^{+}$ molecular ions in the ion source of the mass separator. The previously observed [1]) contaminants ^{20}F and ^{21}O, however, were not detected at mass-48 in this experiment. The resulting γ-singles and the $\gamma\gamma$-coincidence data, compiled in table 1, lead to the partial level scheme shown in fig. 1. The γ-ray energies and the ^{48}Mn level energies were taken from ref. [1]) with the following exceptions:

(i) The intensity of the 1728.8 keV line was determined unambiguously since it was not obscured by the 1730 keV line of the ^{21}O decay.

(ii) The 5040.5 keV line was shown to be entirely due to summing.

(iii) The $\gamma\gamma$-coincidence information is more complete (see table 1), confirming the 9 excited ^{48}Cr levels identified already in the previous experiment [1]).

(iv) Since the energy difference of the newly observed γ-rays of 3750.0 and 4856.1 keV corresponds to the known 1106 keV γ-transition deexciting the lowest 4^{+} state at 1858 keV, they were ascribed to ^{48}Mn decay feeding a new ^{48}Cr level at 5608 keV. This assignment is tentative, as coincidence relations with the 752 and 1106 keV transitions, respectively, were not detected and also no unambiguous grow-in/decay pattern was measured for these two lines.

TABLE 1

Gamma-rays from the ^{48}Mn decay. The γ-intensity values have been corrected for $\gamma\gamma$-coincidence summing on the basis of the experimentally deduced level scheme, the maximum correction amounting to 5.4% for the 1729 keV line. The absolute γ-intensities are given per 100 decays of ^{48}Mn, taking the measured branching ratio of 0.280 (37)% for beta-delayed proton emission into account and neglecting the γ-intensity mismatch (see text)

Energy (keV)	Absolute γ-intensity	Coincident γ-rays
531.0 (5)	0.52 (11)	511, 1106
752.1 (2)	99.7 (60)	511, 760, 1106, 1140, 1364, 1675, 3676, 3901, 3934, 4280
760.2 (2)	3.30 (24)	511, 752, 4280
1106.1 (2)	39.2 (24)	511, 752, 3934
1139.7 (2)	6.49 (44)	511, 752, 3901
1364.0 (2)	21.9 (14)	511, 752, 3676
1675.0 (4)	2.11 (14)	511, 752, 1106, 2259
1728.8 (5)	1.30 (18)	511, 531, 752, 1106
2259.2 (5)	1.60 (19)	511
2570.2 (5)	1.58 (18)	511, 752
3174.1 (5)	2.25 (31)	511, 752
3435.5 (6)	3.19 (38)	511, 752, 1106
3676.2 (4)	30.4 (19)	511, 752, 1364
3750.0 (6)	1.09 (20)	
3900.5 (5)	10.44 (69)	511, 752, 1140
3934.1 (5)	22.9 (16)	511, 752, 1106
4280.1 (5)	9.09 (56)	511, 752, 760
4856.1 (6)	0.54 (10)	511

The γ-ray intensities obtained from this work are listed in table 1. Again, as in the previous experiment [1]), they lead to a mismatch of the intensity balance: The 752 keV level, whose deexciting γ-transition is normalized to 99.7 (60)%, is fed by γ-rays with a total strength of only 89.8 (60)%. Such a discrepancy, if statistically significant, would shed doubts e.g. on the reliability of measured γ-intensities and of deduced beta-decay branching ratios and *ft* values. However, as in the earlier investigation [1]), this mismatch of (9.9 ± 11.4)% is not significantly different from zero and will therefore be neglected in the following without renormalizing the beta intensity. The small γ-intensity difference (0.78 ± 0.19)% between feeding and depopulation of the 4064 keV level will be neglected, too.

The beta-decay branching ratios $I_{\beta+}$ (in percent per ^{48}Mn decay), as deduced from γ data for ^{48}Cr levels up to 5.8 MeV excitation energy, are shown in fig. 1. The *ft* values, given also in fig. 1, are calculated using these I_{β^+} values, the measured half-life of 158.1 (22) ms (see fig. 2), and the *f*-function [9]) based on an estimated ^{48}Mn *Q*-value of 13626 (31) keV. The latter result is obtained as a difference between the measured mass excess of ^{48}V [ref. [10])] and the mass excess of -29192 (30) keV for ^{48}Mn derived from the quadratic form of the isobaric multiplet mass equation [11]).

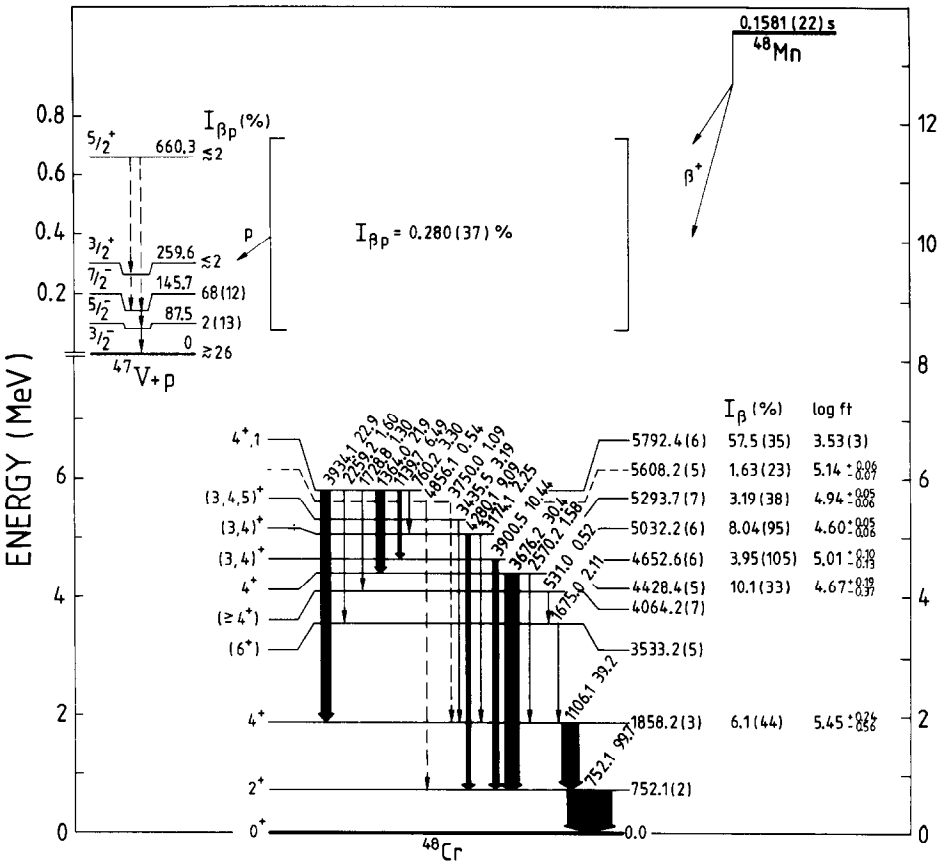

Fig. 1. Partial schemes of ^{47}V and ^{48}Cr levels fed in the decay of ^{48}Mn. The ^{48}Cr levels and the ground-states of ^{48}Mn and ^{47}V are displayed in a common energy scale, whereas an enlarged scale applies for the excited states of ^{47}V. The low-lying excited states of ^{47}V are taken from the literature [8]). Full-drawn γ transitions represent firm assignments made in the present work, while dashed ones mark cases of upper intensity limits (^{47}V) or tentative assignment (^{48}Cr). For comparison of ^{48}Cr levels, identified in ^{48}Mn decay measurements, with reaction data see also ref. [1]) and references therein.

The measured ^{48}Mn half-life of 158.1 (22) ms (see fig. 2) represents a considerable improvement of the previously obtained value of 150 (10) ms [ref. [1])]. In order to check the method used for half-life determination, the decay of ^{20}F with a well-known half-life of 11.00 (2) s [ref. [12])] was also investigated. The mass-47 beam, including ^{20}F as the molecular ion ^{27}Al ^{20}F (see above), was collected for 16 s in the same detector set-up used to obtain the ^{48}Mn half-life data, the collected activity was measured in multispectrum mode (γ-energy range 0–2.6 MeV, 64 1024-channel subgroups, 1.5 s counting time/subgroup), and the mass-47 source was removed subsequently. From 50 such cycles, a ^{20}F half-life of 10.68 (32) s was obtained from analysing the 1634 keV γ-ray. This agreement with the literature value confirms the

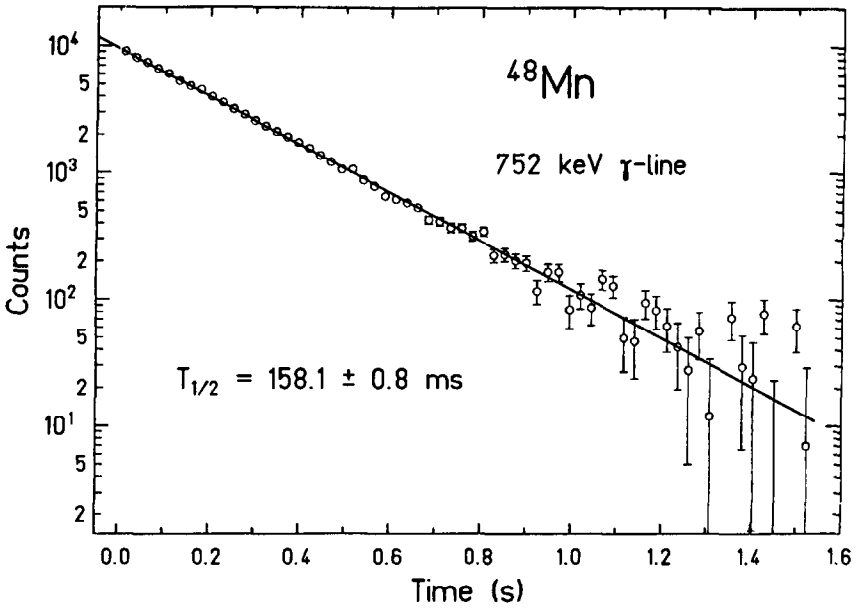

Fig. 2. Decay of the 752 keV γ-ray obtained with a germanium detector. The mass-separated ^{48}Mn beam was collected for 0.4 s on a tape in front of the detector, the decay was then measured for 64 time intervals of 24 ms each, and the activity was removed subsequently from the collector/detector position. 90400 such grow-in/decay/transport cycles were accumulated. The data points represent differences between energy windows on photopeak and background, and the straight line gives the result from a least squares fit assuming one decay component. The statistical error, derived from this fit, amounted to ±0.8 ms (0.5%). The total uncertainty of the ^{48}Mn half-life, however, was estimated to be ±2.2 ms (1.4%), taking into account also the influence of, e.g., dead-time corrections and contributions from long-lived activity.

reliability of the applied method at a level of 3%, it does not prove, however, that the experimental uncertainty of ±1.4%, assigned to the ^{48}Mn half-life (see fig. 2), is free of systematical errors.

The energy spectrum of beta-delayed protons from the ^{48}Mn decay, displayed in fig. 3, shows a peculiar shape with a peak around 1.17 MeV, whose width is close to the instrumental energy resolution of the telescope, and with 4 regularly spaced broad structures between 1.3 and 2.1 MeV. Due to the limited statistics of the proton-energy spectrum and the even more limited statistics of the proton-γ coincidence data, it is difficult to draw conclusions from these details of the spectral shape. There is a good general agreement with respect to intensity and overall-shape between the measured proton-energy spectrum and results obtained from a statistical model [13]) assuming a constant beta strength function (see fig. 3). Concerning the detailed structure, it is interesting to note, that from a fluctuation analysis [13]) one would estimate 9 peaks to occur per 1 MeV interval, which is in qualitative agreement with the experiment.

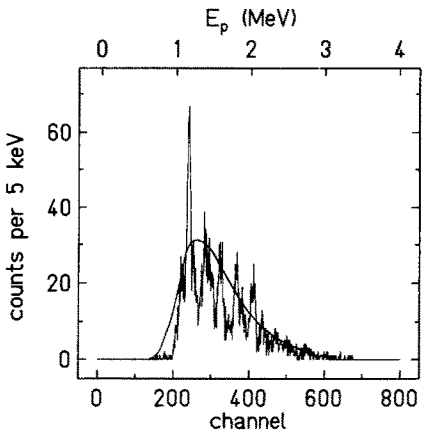

Fig. 3. Measured energy spectrum of beta-delayed protons from the decay of ^{48}Mn, obtained by summing coincident events from a telescope which consisted of a 15.6 μm, 150 mm^2 ΔE and a 531 μm, 450 mm^2 E detector. The counting statistics of this spectrum, shown in histogram form, represents an order-of-magnitude improvement over the previous measurement [1]). The energy spectrum from a statistical-model calculation is also given.

By comparing the simultaneously measured intensities of protons and 752 keV γ-rays and correcting for the detection efficiencies (see sect. 2), the beta-delayed proton branching ratio was determined to be 0.280 (37)% per ^{48}Mn decay.

The γ-ray spectrum, measured in coincidence with the two proton telescopes, is shown in fig. 4. In addition to the proton-coincident 511 keV annihilation radiation due to positron emission from ^{48}Mn decay, two γ-rays of 58.3 and 87.6 keV were clearly observed. These lines are known to be transitions between the lowest lying ^{47}V levels [8]). In deducing branching ratios for proton emission to these levels, the

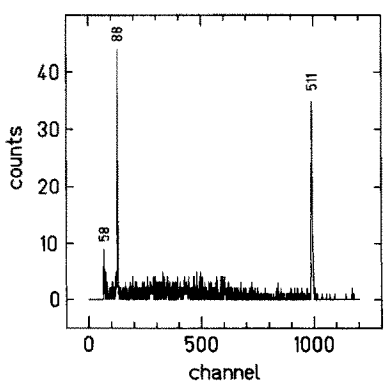

Fig. 4. Energy spectrum of γ-rays measured in coincidence with beta-delayed protons from the ^{48}Mn decay.

sharp decrease of the coincidence efficiency of the germanium detector for low-energy γ-rays was taken into account. Due to this energy dependence, the proton-coincidence correlation is of comparable strength for the two low-energy γ-rays, even though the intensity observed for the 58.3 keV line is much weaker than that measured for the 87.6 keV one. The resulting dominant proton feeding of 68 (12)% to the $\frac{7}{2}^-$, 146 keV level in ^{47}V and the data obtained on feeding of other ^{47}V levels are shown in fig. 1.

Unfortunately, the proton-γ coincidence data did not allow any more detailed conclusion, e.g. on the ^{47}V feeding pattern of restricted proton-energy regions such as the 1.17 MeV peak. In order to deduce ^{48}Mn beta-decay branching ratios from the measured proton intensities, they were integrated over 250 keV intervals. (The channel widths during the measurement was 5 keV, see fig. 3.) The corresponding ^{48}Cr excitation energies (between 8.9 and 11.6 MeV) were determined by summing the respective proton energy from experiment, the proton separation energy of ^{48}Cr (8103 (7) keV [ref. [14])], and the excitation energy of 146 keV of the $\frac{7}{2}^-$ level in ^{47}V. From proton intensities per 250 keV interval, *ft* values were then obtained using half-life and *f*-function as mentioned above for the γ-ray evaluation. The resulting *ft* values above 9.4 MeV excitation energy lie in the range between 4.6 and 4.9.

The *ft* value of an allowed beta-transition can be written as [see ref. [1]) and references therein]

$$ft = (K/g_V'^2)/\{B(F) + (g_A/g_V')^2 B(GT)\}\,, \tag{1}$$

$$K/g_V'^2 = 6170\,(4)\ \text{s}\,, \tag{2}$$

$$|g_A/g_V'| = 1.251\,(9)\,. \tag{3}$$

g_V' and g_A are the effective weak vector coupling constant and the weak axial-vector coupling constant, respectively. The reduced transition probabilities B(F) and B(GT) for Fermi and GT decays are given in units of $g_V'^2/4\pi$ and $g_A^2/4\pi$, respectively.

The values of the constants, given in the eqs. (2) and (3), are taken from the work of Wilkinson *et al.* [15]) and were used e.g. in ref. [2]). We note that somewhat different values, namely $K/g_V'^2 = 6160\,(5)$ s and $|g_A/g_V| = 1.263\,(6)$, are used in ref. [17]) for the discussion of GT transitions near ^{100}Sn and ^{146}Gd (see e.g. ref. [16])), and that data on recent precision measurements of these constants can be found in ref. [18]).

The branching ratio of 57.5 (35)%, measured for the decay of ^{48}Mn to its isobaric analogue state (IAS) in ^{48}Cr, corresponds to a log *ft* value of 3.53 (3). The relative error of ±6.6% for this *ft* value is due to the uncertainties of the branching ratio (±6.1%) and the half-life (±1.4%), and includes also the influence of the *Q*-value error on the *f*-function (±2.1%). From this result, one could in principle obtain g_V' according to eqs. (1), (2), and the relation

$$B(F) = T(T+1) + T_{Z_i} T_{Z_f} \tag{4}$$

which yields $B(F) = 2$ in the ^{48}Mn case [1]). However, the experimental uncertainty of ±6.6% for this *ft* value is far beyond the precision of a few parts in 10^4, reached in g'_V determination from studies of superallowed $0^+ \to 0^+$ decays [18]). It is therefore not meaningful, to use the presently available ^{48}Mn decay data for deriving a g'_V value and for clarifying a possible dependence of this constant on nuclear spin (see discussion in ref. [1])). However, it is interesting to note that the measured *ft* value for the ^{48}Mn decay to the IAS corresponds to a $B(F)$ value which is lower by about 10% than the expected value of 2. Even though this difference is statistically significant only at a level of 1.5 standard deviations and represents therefore at best weak evidence for isospin-forbidden contributions from Fermi decay to other (neighbouring) levels. The latter effect was neglected in deriving $B(GT)$ (see fig. 5a) from the six *ft* values measured for GT decay of ^{48}Mn (see fig. 1).

Shell-model calculations were performed using wave functions for ^{48}Mn and ^{48}Cr obtained in the truncated basis $(0f_{7/2})^{n-r}$ $(0f_{5/2}, 1p_{3/2}, 1p_{1/2})^r$ with $n = 8$ and $r = 0, 1$. The J-T dimensions in this basis go up to about 400 for the 5^+ $T = 1$ state. It would

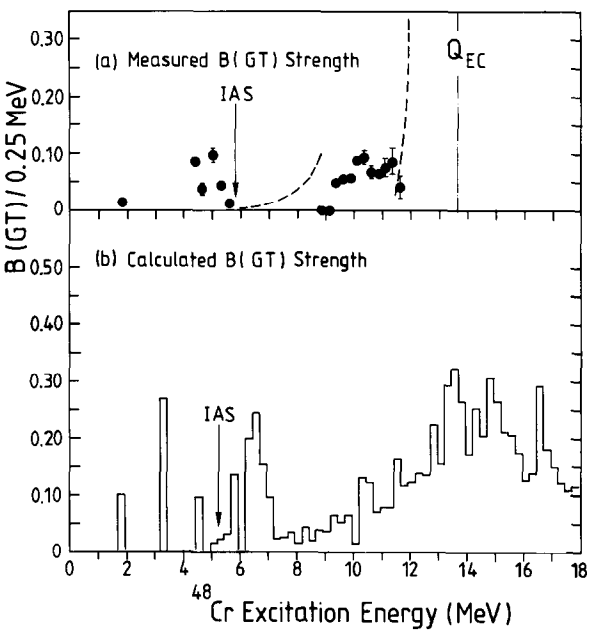

Fig. 5. Comparison of the measured (a) and calculated (b) $B(GT)$ strength for the ^{48}Mn decay. The dashed curves give the sensitivity limits, below which decay strength is expected to remain unobserved in the present experiment. The dash-dotted line marked Q_{EC} represents the upper energy limit of the ^{48}Mn β^+/EC decay, showing that the experiment can only probe the low-energy tail of the (collective) GT giant resonance which apparently is situated at excitation energies of about 15 MeV (see part (b) of the figure). The label IAS indicates the position of the isobaric analogue state in ^{48}Cr. The calculation is based on the FPT interaction (see text). The $B(GT)$ strength is integrated over 250 keV excitation energy intervals, except for level energies up to 5.75 MeV in part (a), which were measured with 0.2–0.7 keV accuracies.

be desirable to include other 1p0f shell configurations, however, the dimensions become too large for practical calculations. We adopt two new interactions derived from fits of the parameters of the modified-surface one-boson exchange potential (MSOBEP) [19]) to 1p0f shell binding energies and excitation energies. One of these, denoted by FPT, was designed to be used with the type of truncation assumed above [20]). The FPT interaction was obtained from a fit to levels in nuclei with $A = 41$–58 which are assumed to be dominated by the $r = 0, 1$ configurations. The other interaction, denoted by FPF, was designed to be used in the full 1p0f basis [21]). The FPF interaction was obtained from a fit to levels in nuclei with $A = 41$–45 which can be diagonalized in the full basis.

The GT strength distribution calculated with the FPT interaction in the truncated basis is compared to experiment in fig. 5. Most of the strength lies in a broad peak centered at 15 MeV which is too high to be observed experimentally. The tail at lower energy is in general agreement with experiment. The most pronounced difference between experiment and theory is found for the second 4^+ state of ^{48}Cr. The experimental energy of 4.428 MeV is in better agreement with the FPT result (3.36 MeV) than with the FPF one (2.66 MeV). However, with both interactions the $B(GT)$ value is relatively large and exceeds by far the experimental one (0.088). The resulting GT quenching factors based on the FPT interaction and averaged over ^{48}Cr excitation-energy intervals of 0–5.75 and 8.75–11.75 MeV, are 0.46 (3) and 0.76 (12), respectively. The low-energy value has been determined previously [1]) to be 0.53 (17) from comparison with shell-model calculations based on the van Hees-Glaudemans interaction, whereas GT quenching for the higher ^{48}Cr excitation-energy range is deduced in this work for the first time. These averaged quenching factors have of course only limited significance in view of the discrepancy between measured and predicted level energies. In spite of this energy mismatch, it is still an interesting question why the $B(GT)$ strength predicted for ^{48}Cr excitation energies around 6.5 MeV was not observed in the experiment.

The same type of energy shift between the experiment and the calculations, which is observed for the second 4^+ state of ^{48}Cr, is also seen for the IAS: The measured value of 5.792 MeV is better reproduced with the FPT interaction which yields 5.26 MeV compared to 3.96 MeV obtained with the FPF interaction. The consistency of this level-energy mismatch, found with both interactions as well as with the interaction we have used previously [1]), indicates that it is probably the model-space truncation which is at fault. As already noted in our previous paper [1]), in the larger model space the 0^+ ground-state should be lowered in binding energy relative to the second 4^+ state and the IAS. With advances in shell-model programs and computer technology it should soon be possible to carry out the calculations in the full 1p0f basis.

The conclusion concerning the relation between energy mismatch and model space can be checked by examining a similar situation in the 1s0d shell, namely the beta decay of the ^{24}Al 4^+ state to states in ^{24}Mg. The GT matrix elements from the

full 1s0d-shell wave functions based on the universal 1s0d shell (USD) interaction of Wildenthal [22]) have been reported previously [2]) and are in good agreement with experiment [2]). We have repeated the calculation with the USD interaction in the truncated basis $(0d_{5/2})^{n-r}\ (0d_{3/2}, 1s_{1/2})^r$ with $n=6$ and $r=0, 1$. We find that the excitation energy of the 4^+ $T=1$ IAS state of ^{24}Mg is lowered from 9.2 MeV in the full basis to 7.1 MeV in the truncated basis. Also, the strongest low-lying GT transition which is concentrated in the third 4^+ $T=0$ state at 8.1 MeV in the full-basis calculation, is shifted down to the second 4^+ $T=0$ state at 6.2 MeV in the truncated basis. This comparison between the full and truncated basis in the 1s0d-shell, using one and the same (USD) interaction, indicates that too small calculated level energies (and a shift of the calculated GT strength towards lower excitation energies) result from the limited truncation. Taking this result together with the similar comparison described above for the $^{48}Mn \rightarrow {}^{48}Cr$ decay, the conclusion is that the quantitative aspects of beta decay are very sensitive to the basis truncation. It would be interesting to see if other approximations such as the QRPA or the Nilsson model can describe the data at this quantitative level.

The authors are indebted to K. Hanold and M.M. Mohar for their support during the measurements, and to C. Bruske, K. Burkard, and W. Hüller for operating the on-line separator.

References

1) T. Sekine, J. Cerny, R. Kirchner, O. Klepper, V.T. Koslowsky, A. Płochocki, E. Roeckl, D. Schardt, B. Sherrill and B.A. Brown, Nucl. Phys. **A467** (1987) 93
2) B.A. Brown and B.H. Wildenthal, At. Data Nucl. Data Tables **33** (1985) 347
3) H. Miyatake, K. Ogawa, T. Shinozuka and M. Fujioka, Nucl. Phys. **A470** (1987) 328
4) M.J.G. Borge, P.G. Hansen, B. Jonson, S. Mattsson, G. Nyman, A. Richter, K. Riisager and the ISOLDE Collaboration, Z. Phys. **A332** (1989) 413
5) J. Honkanen, V. Koponen, P. Taskinen, J. Äystö, K. Eskola, S. Messelt and K. Ogawa, Nucl. Phys. **A496** (1989) 462
6) T. Shinozuka, M. Fujioka, M. Wada, H. Ikegami, H. Sunaoshi, H. Hama, H. Miyatake and K. Ogawa, in Proc. of Yamada Conf. XXIII on nuclear weak process and nuclear structure, Osaka, Japan, 1989, ed. M. Morita, H. Ejiri, H. Otsubo and T. Sato (World Scientific, Singapore, 1989) p. 342
7) R. Kirchner, O. Klepper, D. Marx, G.-E. Rathke and B. Sherrill, Nucl. Instr. Meth. **A247** (1986) 265
8) M.L. Halbert, Nucl. Data Sheets **22** (1977) 59
9) N.B. Gove and M.J. Martin, At. Data Nucl. Data Tables **10** (1971) 205
10) A.H. Wapstra, G. Audi and R. Hoekstra, At. Data Nucl. Data Tables **39** (1988) 281
11) G. Audi and A.H. Wapstra, private communication (1990)
12) F. Ajzenberg-Selove, Nucl. Phys. **A475** (1987) 1
13) B. Jonson, E. Hagberg, P.G. Hansen, P. Hornshøj and P. Tidemand-Petersson, in Proc. 3rd Int. Conf. on nuclei far from stability, Cargése, France, 1976, CERN 76-13 (1976), p. 277
14) A.H. Wapstra and G. Audi, Nucl. Phys. **A432** (1985) 1
15) D.H. Wilkinson and B.E.F. Macefield, Nucl. Phys. **232** (1974) 58
16) O. Klepper and K. Rykaczewski, in Proc. Predeal Int. Summer School. Recent advances in nuclear structure, Predeal, Romania, 1990

17) I.S. Towner and J.C. Hardy, in Proc. 7th Int. Conf. on atomic masses and fundamental constants, Darmstadt-Seeheim, 1984, ed. O. Klepper, THD-Schriftenreihe Wissenschaft und Technik **26** (TH Darmstadt, 1984) p. 564
18) J.C. Hardy, I.S. Towner, V.T. Koslowsky, E. Hagberg and H. Schmeing, Nucl. Phys. **A509** (1990) 429
19) B.A. Brown, W.A. Richter, R.E. Julies and B.H. Wildenthal, Ann. of Phys. **182** (1988) 191
20) W.A. Richter, M.G. van der Merwe and B.A. Brown, in Proc. 3rd Int. Spring Meeting on nuclear physics: Understanding the variety of nuclear excitations, ed. A. Covello (World Scientific, Singapore, 1990) to be published
21) W.A. Richter, M.G. van der Merwe, R.E. Julies, B.A. Brown and L. Zhao, in Proc. 2nd Int. Spring Meeting on nuclear physics: Shell model and nuclear structure: Where do we stand?, ed. A. Covello (World Scientific, Singapore, 1989) p. 149; and submitted to Nucl. Phys. **A**
22) B.H. Wildenthal, Prog. Part. Nucl. Phys. **11** (1984) 5